

Failure of an Automobile Rear Axle

* INTRODUCTION

* TESTING PROCEDURE AND RESULTS

* Impact Tests

* Tensile Tests

INTRODUCTION

Subsequent to an accident in which a light pickup truck left the road and overturned, it was noted that one of the rear axes had failed at a point near the wheel mounting flange. This axle was made of a **steel** that contained approximately **0.3 wt% C**. Furthermore, the other axle was intact and did not experience fracture. An **investigation** was carried out to determine whether **the axle failure caused the accident** or whether **the failure occurred as a consequence of the accident**.

Figure 22.11 is a schematic diagram that shows the components of a rear axle assembly of the type used in this pickup truck. The fracture occurred adjacent to the bearing lock nut, as noted in this schematic.

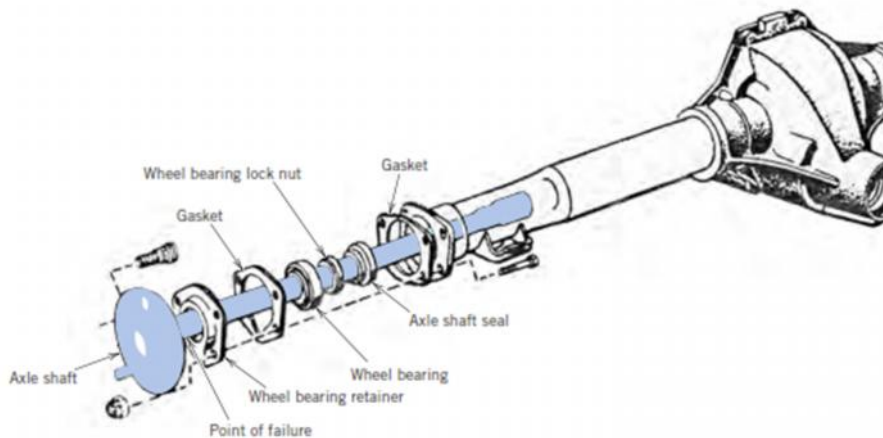


Figure 22.11 Schematic diagram showing typical components of a light truck axle, and the fracture site for the failed axle of this case study. (Reproduced from *MOTOR Auto Repair Manual*, 39th Edition © Copyright 1975. By permission of the Hearst Corporation.)

Upon examination of the fracture surface it was noted that the region corresponding to the outside shaft perimeter [being approximately 6.4 mm (0.25 in.) wide] was very flat; furthermore, the center region was rough in appearance.

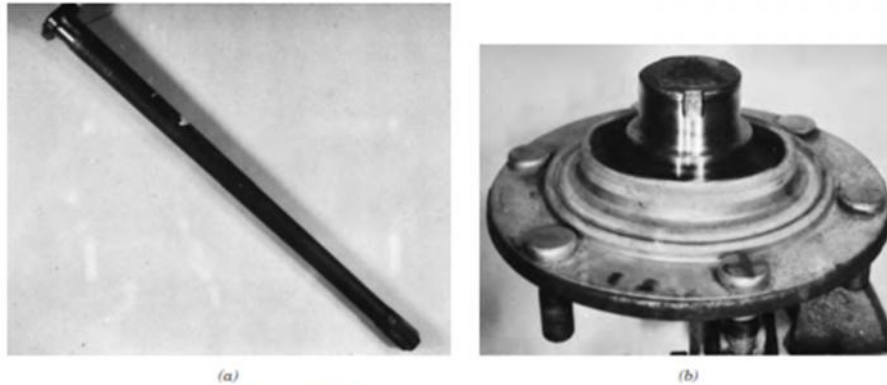


Figure 22.12 (a) Photograph of one section of the failed axle. (b) Photograph showing wheel mounting flange and stub end of failed axle. [Reproduced with permission from *Handbook of Case Studies in Failure Analysis, Vol. 1* (1992), ASM International, Materials Park, OH, 44073-0002.]

TESTING PROCEDURE AND RESULTS

Details of the fracture surface in the vicinity of the keyway are shown in the photograph of Figure 22.13; note that the keyway appears at the bottom of the photograph. Both the flat outer perimeter and rough interior regions may be observed in the photograph. There are **chevron patterns** that emanate inward from the corners of and parallel to the sides of the keyway; these are barely discernible in the photograph, but indicate the direction of crack propagation. Fractographic analyses were also conducted on the fracture surface. Figure 22.14 shows a scanning electron micrograph taken near one of the keyway corners. Cleavage features may be noted in this micrograph, whereas any evidence of dimples

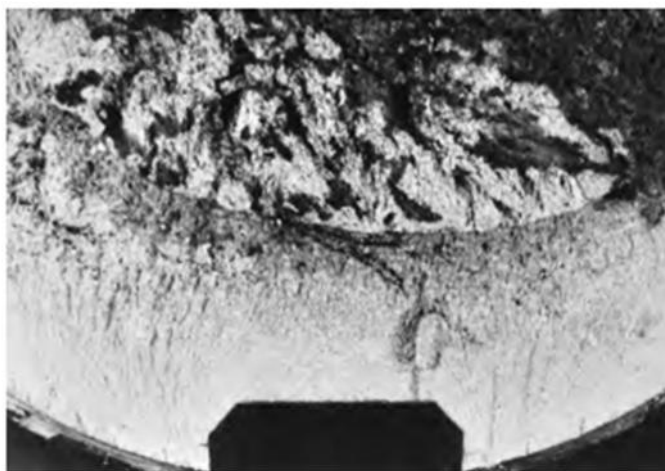


Figure 22.13 Optical micrograph of failed section of axle that shows the keyway (bottom), as well as the flat outer perimeter and rough core regions. [Reproduced with permission from *Handbook of Case Studies in Failure Analysis, Vol. 1* (1992), ASM International, Materials Park, OH, 44073-0002.]

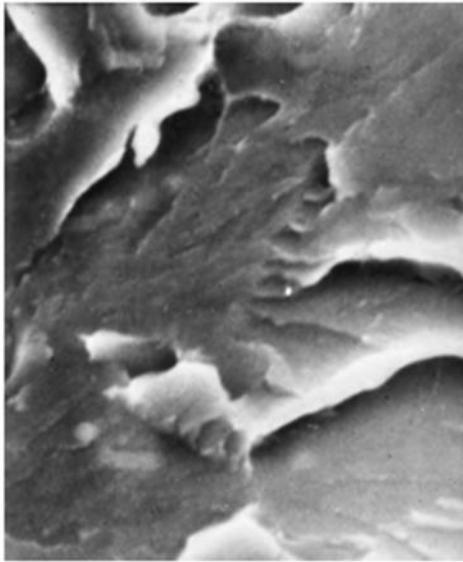


Figure 22.14 Scanning electron micrograph of failed axle outer perimeter region near the keyway, which shows cleavage features. 3500 \times . [Reproduced with permission from *Handbook of Case Studies in Failure Analysis, Vol. 1* (1992), ASM International, Materials Park, OH, 44073-0002.]

and fatigue striations is absent. These results indicate that the mode of fracture within this **outer periphery** of the shaft was **brittle**.

An SEM micrograph taken of **the rough central region** (Figure 22.15) revealed the presence of both **brittle cleavage features and also dimples**; thus, it is apparent that the failure mode in this central interior region was mixed; that is, it was a **combination of both brittle and ductile fracture**.

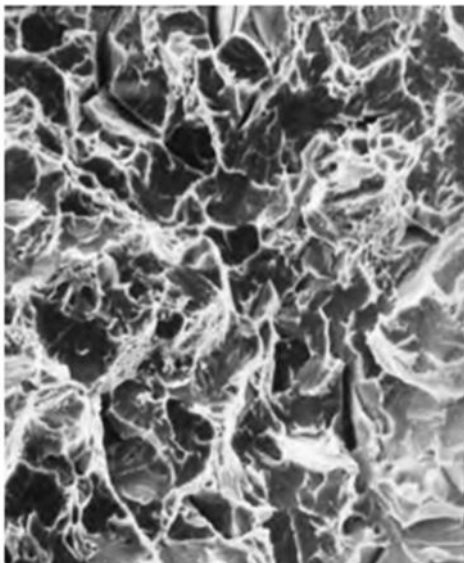


Figure 22.15 Scanning electron micrograph of the failed axle rough central core region, which is composed of mixed cleavage and dimpled regions. 570 \times . [Reproduced with permission from *Handbook of Case Studies in Failure Analysis, Vol. 1* (1992), ASM International, Materials Park, OH, 44073-0002.]

Metallographic examinations were also performed. A transverse cross section of the failed axle was polished, etched, and photographed using the **optical microscope**. The microstructure of the outer periphery region, as on the other hand, in the central region the microstructure was completely different; from Figure 22.17, shown in Figure 22.16, consisted of tempered martensite.

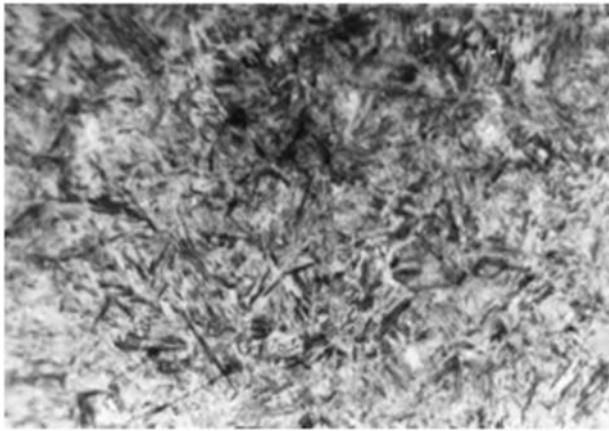
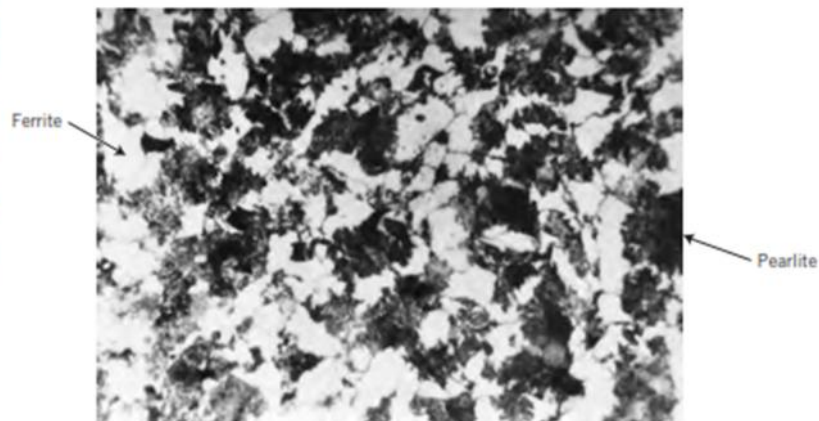


Figure 22.16 Optical photomicrograph of the failed axle outer perimeter region, which is composed of tempered martensite. 500×. [Reproduced with permission from *Handbook of Case Studies in Failure Analysis, Vol. 1* (1992), ASM International, Materials Park, OH, 44073-0002.]

A photomicrograph of this region, it may be noted that the microconstituents are ferrite, pearlite, and possibly some bainite.

Figure 22.17 Optical photomicrograph of the failed axle central core region, which is composed of ferrite and pearlite (and possibly bainite). 500×. [Reproduced with permission from *Handbook of Case Studies in Failure Analysis, Vol. 1* (1992), ASM International, Materials Park, OH, 44073-0002.]



In addition, transverse microhardness measurements were taken along the cross section; in Figure 22.18 is plotted the resulting hardness profile. Here it may be noted that the maximum hardness of approximately 56 HRC occurred near the surface, and that hardness diminished with radial distance to a hardness of about 20 HRC near the center. On the basis of the observed microstructures and this hardness profile, it was assumed that the axle had been induction hardened. At this point in the investigation it was not possible to ascertain irrefutably whether the axle fracture caused the accident or whether the accident caused the fracture.

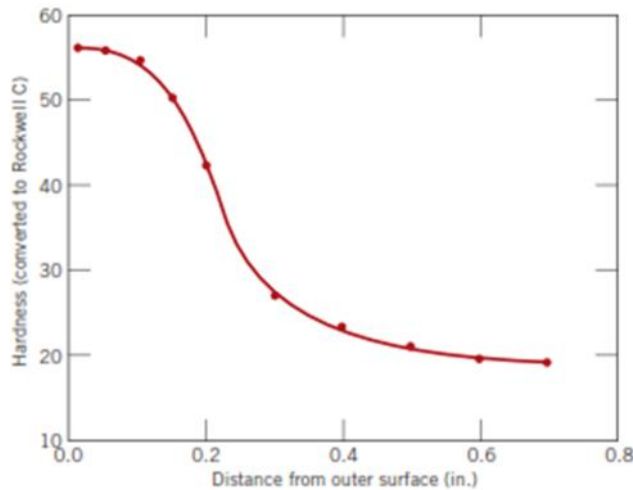


Figure 22.18 Transverse hardness profile across the axle cross section. (Microhardness readings were converted to Rockwell C values). [Reproduced with permission from *Handbook of Case Studies in Failure Analysis, Vol. 1* (1992), ASM International, Materials Park, OH, 44073-0002.]

The high hardness and, in addition, the evidence of cleavage of the outer surface layer indicated that this region failed in a brittle manner as a result of being overloaded (i.e., as a result of the accident). On the other hand, the evidence of a mixed ductile-brittle mode of fracture in the central region neither supported nor refuted either of the two possible failure scenarios.

It was hypothesized that **the central core region was strain-rate sensitive to fracture**; that is, at **high strain rates**, as with the truck rollover, the fracture mode would be **brittle**. By contrast, if failure was due to loads that were applied relatively **slowly**, as under normal driving conditions, the mode of failure would be **more ductile**. In light of this reasoning and, also, in order to glean further evidence as to cause of failure, it was decided to fabricate and test both impact and tensile specimens.

Impact Tests

For the impact tests, small [2.5 mm (0.1 in.) wide] Charpy V-notch test specimens were prepared from both outer perimeter and interior areas. Since the hardened outer region was very thin (6.4 mm thick), careful machining of these specimens was required. Impact tests were conducted at room temperature, and it was noted that the energy absorbed by the surface specimen was significantly lower than for the core specimen [4 J (3 ft-lbf) versus 11 J (8 ft-lbf)].

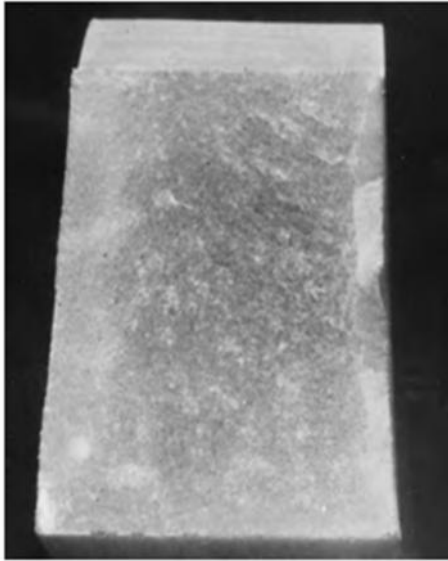


Figure 22.19 Fracture surface of the Charpy impact specimen that was taken from the outer perimeter region. [Reproduced with permission from *Handbook of Case Studies in Failure Analysis, Vol. 1* (1992), ASM International, Materials Park, OH, 44073-0002.]

Furthermore, the appearances of the fracture surfaces for the two specimens were dissimilar. Very little, if any, deformation was observed for the outer perimeter specimen (Figure 22.19); conversely, the core specimen deformed significantly (Figure 22.20).



Figure 22.20 Fracture surface of the Charpy impact specimen that was taken from the central core region. [Reproduced with permission from *Handbook of Case Studies in Failure Analysis, Vol. 1* (1992), ASM International, Materials Park, OH, 44073-0002.]

Fracture surfaces of these impact specimens were then subjected to examination using the SEM.

Figure 22.21, a micrograph of the outer-periphery specimen that was impact tested, reveals the presence of cleavage features, which indicates that this was a brittle fracture.

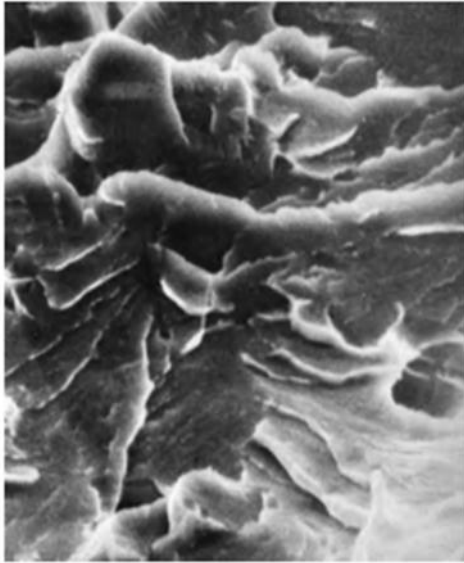
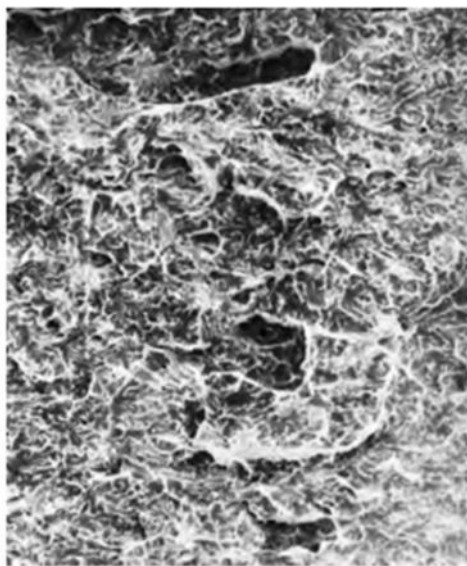


Figure 22.21 Scanning electron micrograph of the fracture surface for the impact specimen prepared from the outer perimeter region of the failed axle. 3000 \times . [Reproduced with permission from *Handbook of Case Studies in Failure Analysis, Vol. 1* (1992), ASM International, Materials Park, OH, 44073-0002.]

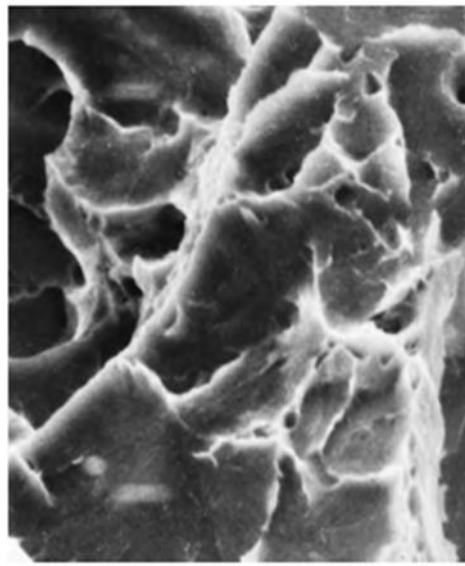
Furthermore, the morphology of this fracture surface is similar to that of the actual failed axle (Figure 22.14).

For the impact specimen taken from the center-core region the fracture surface had a much different appearance; Figures 22.22a and 22.22b show micrographs for this specimen, which were taken at relatively low and high magnifications, respectively.

These micrographs reveal the details of this surface to be composed of interspersed **cleavage features and shallow dimples**, being similar to the failed axle, as shown in Figure 22.15. Thus, the fracture of this specimen **was of the mixed-mode type**, having both ductile and brittle components.



(a)



(b)

Figure 22.22 (a) Scanning electron micrograph of the fracture surface for the impact specimen prepared from the center-core region of the failed axle. 120 \times . (b) Scanning electron micrograph of the fracture surface for the impact specimen prepared from the center-core region of the failed axle taken at a higher magnification than (a); interspersed cleavage and dimpled features may be noted. 3000 \times . [Reproduced with permission from *Handbook of Case Studies in Failure Analysis, Vol. 1* (1992), ASM International, Materials Park, OH, 44073-0002.]

Tensile Tests

A tensile specimen taken from the **center-core region** was pulled in tension to failure. The fractured specimen displayed the **cup-and-cone** configuration, which indicated at least a **moderate level of ductility**.

A fracture surface was examined using the SEM, and its morphology is presented in the micrograph of Figure 22.23. The

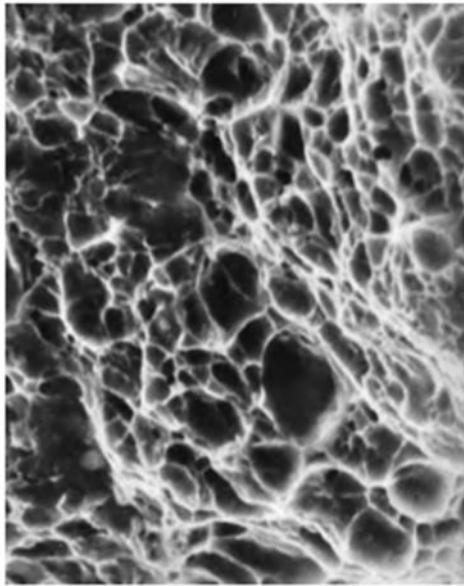


Figure 22.23 Scanning electron micrograph of the fracture surface for the inner-core specimen that was tensile tested; a completely dimpled structure may be noted. Approximately 3500 \times . [Reproduced with permission from *Handbook of Case Studies in Failure Analysis, Vol. 1* (1992), ASM International, Materials Park, OH, 44073-0002.]

The surface was composed entirely of dimples, which confirms that this material was at least moderately ductile and that there was no evidence of brittle fracture. Thus, although this center-core material exhibited mixed-mode fracture under impact loading conditions, when the load was applied at a relatively slow rate (as with the tensile test), failure was highly ductile in nature.

DISCUSSION

In light of the previous discussion it was supposed that the truck rollover was responsible for the axle failure. Reasons for this supposition are as follows:

1. The outer perimeter region of the failed axle shaft failed in a brittle manner, as did also the specimen taken from this region that was impact tested. This conclusion was based on the fact that both fracture surfaces were very flat, and that SEM micrographs revealed the presence of cleavage facets.
2. The fracture behavior of the **central core** region was **strain-rate sensitive**, and indicated that **axle failure** was due to a **single high strain-**



rate incident. Fracture surface features for both the failed axle and impact-tested (i.e., high strain-rate-tested) specimens taken from this core region were similar: SEM micrographs revealed the presence of features (cleavage features and dimples) that are characteristic of mixed mode (brittle and ductile) fracture.

In spite of evidence supporting the validity of the accident-caused-axle-failure scenario, the plausibility of the other (axle-failure-caused-the-accident) scenario was also explored. This latter scenario necessarily assumes that a fatigue crack or some other slow-crack propagation mechanism initiated the sequence of events that caused the accident. In this case it is important to consider the mechanical characteristics of that portion of the specimen that was last to fail—in this instance, the core region. If failure was due to fatigue, then any increase in loading level of this core region would have occurred relatively slowly, not rapidly as with impact loading conditions.

During this gradually increasing load level, fatigue crack propagation would have continued until a critical length was achieved (i.e., until the remaining intact axle cross section was no longer capable of sustaining the applied load); at this time, final failure would have occurred.

On the basis of the tensile tests (i.e., slow strain-rate tests) performed on this core region, the appearance of the axle fracture **surface** would be **entirely ductile** (i.e., dimpled, as per the SEM micrograph of Figure 22.23). Inasmuch as this core region of the failed shaft exhibited mixed (**ductile and brittle**) mode fracture features (**both cleavage features and dimples**, Figure 22.15), and not exclusively dimples, the axle-failure-caused-the-accident scenario was rejected.